

Scientific Inquiry and Review (SIR)

Volume 7 Issue2, 2023

ISSN (P): 2521-2427, ISSN (E): 2521-2435

Homepage: <https://journals.umt.edu.pk/index.php/SIR>



Article QR



Title: Shape-Preserving Curve and Surface Data Embedding Algorithm

Author (s): Farheen Ibraheem¹, Shamaila Samreen², Muhammad Bilal Riaz³, Tayba Arooj⁴

Affiliation (s): ¹Forman Christian College, A Chartered University-FCCU, Lahore-Pakistan

²University of Engineering and Technology- Lahore-Pakistan

³Gdansk University of Technology – Poland

⁴Lahore College for Women University, Lahore, Pakistan

DOI: <https://doi.org/10.32350/sir.72.01>

History: Received: December 08, 2022, Revised: March 20, 2023, Accepted: March 21, 2023,

Published: June 15, 2023

Citation: Ibraheem F, Samreen S, Riaz MB, Arooj T. Shape-Preserving curve and surface data embedding algorithm Pakistan. *Sci Inq Rev.* 2023;7(2):1–37.

<https://doi.org/10.32350/sir.72.01>

Copyright: © The Authors

Licensing: This article is open access and is distributed under the terms of [Creative Commons Attribution 4.0 International License](#)

Conflict of Interest: Author(s) declared no conflict of interest



A publication of
The School of Science
University of Management and Technology, Lahore, Pakistan

Shape-Preserving Curve and Surface Data Embedding Algorithm

Farheen Ibraheem^{1*}, Shamaila Samreen², Muhammad Bilal Riaz³, and Tayba Arooj⁴

¹Forman Christian College, A Chartered University-FCCU, Lahore, Pakistan

²University of Engineering and Technology, Lahore, Pakistan

³Faculty of Applied Physics and Mathematics, Gdansk University of Technology, Poland

⁴Lahore College for Women University, Lahore, Pakistan

ABSTRACT

In this study, shape preserving data driven rational cubic schemes are developed. A rational cubic piecewise function (quadratic denominator and cubic numerator) with two parameters was transformed to C^1 rational cubic piecewise function. Constraints were derived on free parameters by means of some mathematical derivations to train and demonstrate convex curve. The scheme, then, was advanced to partially blended rational bi-cubic function with eight free parameters which were controlled to ascertain convex surface. A numerical comparison with certain existing schemes manifested that the proposed method was economical. The proposed scheme was put into visualization of convex 2D and 3D data using MATLAB software packet. Additionally, the suggested approach produced a more visually appealing interpolating curve for scientific visualization for specific data sets.

Keywords: convex data, convex surface, rational functions, shape preservation

1. INTRODUCTION

A considerable amount of raw data that represents the experiment's outcomes is typically obtained by the scientists when the experiments are carried out in the lab. For instance, the data in a chemical experiment might be the distillation curve, whereas in a biology experiment, it could be the movement of the relevant cell within the system. Additionally, any experiment may have error or noise in the data collecting procedures. The type of error could be systematic, biased, or random. Other methods of data processing, such as data fitting and data smoothing or filtering were applied to these types of data. Interpolation is a preferable alternative for the data if

* Corresponding Author: farheenibraheem@fccollege.edu.pk

Scientific Inquiry and Review

the data is clean, which means there are probably no errors. However, if the data contains noise, approximation, smoothing, or de-noising may be advantageous to gain fruitful results. There are several popular techniques for processing the data including linear regression, polynomial regression (or fitting), any non-polynomial fitting, cubic splines, and smoothing splines. Interpolation, on the other hand, addresses the problem of creating curve or surface that must also maintain the data's geometric shape when it is approximated which is subject of the current research.

Science and engineering, both rely on these continuous visual representations of discrete scientific data in particular which are coherent with intrinsic properties of the data. Computational methods used in these realms are terms as shape preserving algorithms. The design of shape preserving data embedded curves and surfaces lies at the heart of several scientific disciplines in the digital age including computer-aided geometric design (CAGD), computer graphics, and computer-aided design (CAD). These applied areas combine via computational software packets, ideas from numerical techniques, visualization, differential geometry, and linear algebra. Surface and curve drawing schemes offered architects a competitive edge over traditional drafting tool and optimized the likelihood of realizing their ideas by exhibiting their thoughts on computer displays in remarkable short amount of time.

Moreover, the design of machine software, robotics, and chemical processes are among the many fields in which shape-preserving approaches are widely used. For designing ceramics, cutting wood for wooden furniture and creating ornaments, a lathe is utilized. The design of the lathe path is made by using shape-preserving software. Shape-preserving interpolation techniques are employed in both, chemistry and robotics, to plan the path of the robots. In chemistry, they are used for PARFAC modelling of the fluorescence data. There are more applications in the areas of signal processing and photogrammetric data manipulation. Convexity, monotonicity, and positivity are the most dominant data types. All of these applications have to be retained in the process of visualization.

The usual data interpolation algorithms present the data smoothly, however, fail to intact its shapes. The existing shape-preserving algorithms restrain the derivatives at the knots to envisage convex, monotone, and positive data as convex, monotone, and positive surfaces and curves and operate effectively with specific conditions, for instance, the solution of

ordinary and partial differential equations cannot be interpolated by these shape-preserving methods. Another strategy is to add additional knots between the existing data points. Even though these techniques maintain the forms of the data, the amount of computing work has grown larger.

The motivation behind the current research was to devise an efficient and economic algorithm that not only delivers smooth visualizations but confirms convexity in the visual attribute. This research addressed the convex surface and curve interpolation which has become a fundamental element of numerous applications in several areas, such as airplane and automotive industries, architecture, mechanical engineering, and computer graphics. Likewise, convexity in yield curve measures the extent at which price of a bond changes with the rate of interest prevalent in market. It benefits the stakeholders to anticipate price of a bond if market interest rate changes. Furthermore, indifference curve in economics which ranks a consumer's preference for a combination of goods represents convex structure.

Shape conserving convex interpolation was well explored in past few decades and some eminent contributions are [1–26]. The control points of the boundary of 2D shape are optimized using B'ezier curve in [1] and [2]. BFGS diagonal approximation method was employed in [3] to solve B spline curve fitting problem. Surface reconstruction, using B spline and BFGS diagonal approximation, was discussed in [4]. Kvasov [6] presented two algorithms to preserve the monotonicity and convexity of the discrete data by using weighted C^1 quadratic splines. Verlan [7] proposed an algorithm of C^2 interpolation utilizing splines of arbitrary degree for discrete data to achieve the convexity conservation of data. Moreover, in [8–10] convexity preserving techniques were global.

Brodlie and Butt [11] presented a piecewise cubic C^1 interpolant to preserve the convexity of the data. Hussain et al. [12] suggested a local shape preserving interpolation scheme through GC^1 bi-quadratic trigonometric spline. The scheme comprised of four free parameters in each rectangular domain. These free parameters were controlled so that no possible fluctuations could be seen. This scheme maintained the smoothness of positive and monotone 3D data. Sarfraz et al. [14] constructed a rational cubic function with two parameters in the vision of captivating positive data. Simple constraints were manipulated on two parameters in the illustration of rational cubic function and extended rational bi-cubic

partially blended function. The scheme was local with an approximation order of $O(h_i^3)$. Sarfraz et al. [15] developed the smooth shape preserving methods deploying piecewise rational cubic and the rational bi-cubic function to conserve the convexity for 2D and 3D data. The data dependent constraints on free parameters were evaluated to achieve the shape of convex data. The convexity conserving schemes yielded adequate degrees of freedom to facilitate the researcher and user. The convex shape of the data was not preserved by the techniques in [17] when the data was presented with derivatives.

To retain the shape of convex data, Costantini and Fontanella [22] created a semi-global approach. However, this scheme was not economical as degree of interpolant in some rectangular patches became excessively high and the polynomial patches tended to be linear in x and/or y. The resulting surfaces, also, failed to attain a visually pleasant look. In order to create convex surfaces, Asatryan [23] each rectangular grid was divided into nine smaller rectangles. This scheme was not local which means that by altering the data for one sub rectangle's edge in the x direction, a modification was made to the grid for all of the sub rectangle's edges that were originally situated in the x direction. The convex data visualization techniques created in [24] were global.

In [25], the proposed approach kept the convexity of the surface along the grid lines, but failed to preserve the convexity inside the grids, leading to unfavorable flat areas because second order mixed partial derivatives vanished. A univariate C^2 cubic spline was utilized to preserve convexity. A C^2 quartic \ quadratic interpolant was used by authors in [26] to visualize monotone, convex, and positive data set.

The convex shape of the data was not preserved by the techniques in [17, 25] when the data was presented with derivatives.

The main focus of the current paper was to derive data dependent constraints on parameters in the description of piece wise rational cubic and bi-cubic functions in [14] to hold convexity. The research conducted for this purpose was discussed in several sections. Section 2 and Section 3 presents a review of piece wise rational cubic and rational bi-cubic function [14] to be employed. Convexity preserving constraints for curve and surface data were developed in Section 4. Section 5 provides implementation of rational scheme developed on 2D and 3D data sets and corresponding numerical

results were demonstrated in Section 6. Proposed research algorithm was concluded in Section 7.

2. RATIONAL CUBIC FUNCTION

The rational cubic function introduced by Sarfraz et al. [14] is explained in this section.

Suppose that (u_j, v_j) , where $j = 0, 1, 2, \dots, n$ are the set of given data points defined over the interval $[a, b]$ such that $a = u_0 < u_1 < u_2 < \dots < u_n = b$. The piecewise rational cubic function with two parameters ϱ_j and σ_j defined over the each subinterval $I_j = [u_{j+1}, u_j]$ where $j = 0, 1, 2, 3, \dots, n - 1$ is given by:

$$T_j(u) = \frac{P_j(\xi)}{Q_j(\xi)}, \quad (2.1)$$

where

$$P_j(\xi) = \varrho_j v_j (1 - \xi)^3 + \{\varrho_j v_j + h_j \varrho_j d_j + 2v_j\} (1 - \xi)^2 \xi + \{\sigma_j v_{j+1} - h_j \sigma_j d_{j+1} + 2v_{j+1}\} (1 - \xi) \xi^2 + \sigma_j v_{j+1} \xi^3,$$

$$Q_j(\xi) = \varrho_j (1 - \xi)^2 + 2(1 - \xi) \xi + \sigma_j \xi^2,$$

$$\xi = \frac{(u - u_j)}{h_j}, \quad h_j = u_{j+1} - u_j.$$

The rational cubic function defined in **Eq. (2.1)** is C^1 if the following characteristics hold,

$$T_j(u_j) = v_j, \quad T_j(u_{j+1}) = v_{j+1}, \quad T_j^{(1)}(u_j) = d_j, \quad T_j^{(1)}(u_{j+1}) = d_{j+1} \quad (2.2)$$

where $T^{(1)}$ signifies derivative with respect to 'u' and d_j symbolizes the derivative values at the knots u_j . Interestingly, taking $\varrho_j = \sigma_j = 1$, rational cubic spline takes the form of standard cubic Hermite spline in each interval $I_j = [u_j, u_{j+1}]$.

3. RATIONAL BI-CUBIC FUNCTION

In this section, the rational cubic function in **Eq. (2.1)** is expanded to a rational bi-cubic function specified over three-dimensional set of data points $\{(u_j, v_j, \tilde{G}_{j,l}): j = 0, 1, 2, \dots, n; l = 0, 1, 2, \dots, m\}$ with the rectangular

grid $M = [u_0, u_n] \times [v_0, v_m]$. Let $\tilde{\mu}: a = u_0 < u_1 < u_2 < \dots < u_n = b$ be the partition of $[a, b]$ and $\tilde{\pi}: c = v_0 < v_1 < v_2 < \dots < v_n = d$ be the partition of $[c, d]$. The rational bi-cubic partially blended function can be defined over each rectangular patch $I_j = [u_j, u_{j+1}] \times [v_l, v_{l+1}]$ as:

$$T(u, v) = -EGN^T, \quad (3.1)$$

where

$$G = \begin{pmatrix} 0 & T(u, v_l) & T(u, v_{l+1}) \\ T(u_j, v) & T(u_j, v_l) & T(v_j, v_{l+1}) \\ T(u_{j+1}, v) & T(u_{j+1}, v_l) & T(u_{j+1}, v_{l+1}) \end{pmatrix}, \quad (3.2)$$

$$E = [-1 \quad \tau_0(\xi) \quad \tau_1(\xi)],$$

$$N = [-1 \quad \lambda_0(\eta) \quad \lambda_1(\eta)],$$

where

$$\tau_0 = (1 - \xi)^2(1 + 2\xi), \quad \tau_1 = \xi^2(3 - 2\xi), \quad \lambda_0 = (1 - \eta)^2(1 + 2\eta), \quad \lambda_1 = \eta^2(3 - 2\eta).$$

$$\text{Furthermore, } \xi = \frac{(u - u_j)}{h_j} \quad 0 \leq \xi \leq 1, \quad \eta = \frac{(v - v_l)}{\bar{h}_l} \quad 0 \leq \eta \leq 1,$$

$$h_j = u_{j+1} - u_j, \quad \bar{h}_l = v_{l+1} - v_l.$$

The rational cubic function $T(u, v_l), T(u, v_{l+1}), T(u_j, v), T(u_{j+1}, v)$ similar to **Eq. (2.1)** are attained and specified over the boundary of rectangular portion as:

$$T(u, v_l) = \frac{\sum_{l=0}^3 (1 - \xi)^{3-l} \xi^l M_l}{Q_1(\xi)}, \quad (3.3)$$

where

$$M_0 = \varrho_{j,l} \tilde{G}_{j,l},$$

$$M_1 = \varrho_{j,l} \tilde{G}_{j,l} + h_j \varrho_{j,l} \tilde{G}_{j,l}^u + 2 \tilde{G}_{j,l},$$

$$M_2 = \sigma_{j,l} \tilde{G}_{j+1,l} - h_j \sigma_{j,l} \tilde{G}_{j+1,l}^u + 2 \tilde{G}_{j+1,l}, \quad M_3 = \sigma_{j,l} \tilde{G}_{j+1,l}$$

$$Q_1(\xi) = \varrho_{j,l} (1 - \xi)^2 + (1 - \xi) \xi + \sigma_{j,l} \xi^2$$

with $\varrho_{j,l}$ and $\sigma_{j,l}$ shape parameters.

Likewise,

$$T(u, v_{l+1}) = \frac{\sum_{l=0}^3 (1-\xi)^{3-l} \xi^l N_l}{Q_2(\xi)}, \quad (3.4)$$

where

$$\begin{aligned} N_0 &= \varrho_{j,l+1} \tilde{G}_{j,l+1}, N_1 = \varrho_{j,l+1} \tilde{G}_{j,l+1} + h_j \varrho_{j,l+1} \tilde{G}_{j,l+1}^u + 2 \tilde{G}_{j,l+1}, \\ N_2 &= \sigma_{j,l+1} \tilde{G}_{j+1,l+1} - h_j \sigma_{j,l+1} \tilde{G}_{j+1,l+1}^u + 2 \tilde{G}_{j+1,l+1}, N_3 = \sigma_{j,l+1} \tilde{G}_{j+1,l+1}, \\ Q_2(\xi) &= \varrho_{j,l+1} (1-\xi)^2 + (1-\xi)\xi + \sigma_{j,l+1} \xi^2 \end{aligned}$$

with shape parameter $\varrho_{j,l+1}$ and $\sigma_{j,l+1}$.

Further, we have,

$$T(u_j, v) = \frac{\sum_{j=0}^3 (1-\eta)^{3-j} \eta^j J_j}{Q_3(\eta)}, \quad (3.5)$$

where

$$\begin{aligned} J_0 &= \bar{\varrho}_{j,l} \tilde{G}_{j,l}, J_1 = \bar{\varrho}_{j,l} \tilde{G}_{j,l} + \bar{h}_j \bar{\varrho}_{j,l} \tilde{G}_{j,l}^u + 2 \tilde{G}_{j,l}, \\ J_2 &= \bar{\sigma}_{j,l} \tilde{G}_{j,l+1} - \bar{h}_j \bar{\sigma}_{j,l} \tilde{G}_{j,l+1}^u + 2 \tilde{G}_{j,l+1}, J_3 = \bar{\sigma}_{j,l} \tilde{G}_{j,l+1}, \\ Q_3(\eta) &= \bar{\varrho}_{j,l} (1-\eta)^2 + (1-\eta)\eta + \bar{\sigma}_{j,l} \eta^2 \end{aligned}$$

with shape parameter $\bar{\varrho}_{j,l}$ and $\bar{\sigma}_{j,l}$.

Lastly,

$$T(u_{j+1}, v) = \frac{\sum_{j=0}^3 (1-\eta)^{3-j} \eta^j K_j}{Q_4(\eta)}, \quad (3.6)$$

where

$$\begin{aligned} K_0 &= \bar{\varrho}_{j+1,l} \tilde{G}_{j+1,l}, K_1 = \bar{\varrho}_{j+1,l} \tilde{G}_{j+1,l} + \bar{h}_j \bar{\varrho}_{j+1,l} \tilde{G}_{j+1,l}^u + 2 \tilde{G}_{j+1,l}, \\ K_2 &= \bar{\sigma}_{j+1,l} \tilde{G}_{j+1,l+1} - \bar{h}_j \bar{\sigma}_{j+1,l} \tilde{G}_{j+1,l+1}^u + 2 \tilde{G}_{j+1,l+1}, K_3 = \bar{\sigma}_{j+1,l} \tilde{G}_{j+1,l+1}, \\ Q_4(\eta) &= \bar{\varrho}_{j+1,l} (1-\eta)^2 + (1-\eta)\eta + \bar{\sigma}_{j+1,l} \eta^2 \end{aligned}$$

With shape parameters $\bar{\varrho}_{j+1,l}$ and $\bar{\sigma}_{j+1,l}$.

4. THE PROPOSED ALGORITHM

This section uses the rational cubic function and rational bi-cubic function to build convexity-preserving for regular surface data (2).

4.1. Convex Curve Model

Assume that $\{(u_j, v_j); j = 0, 1, 2, \dots, n\}$ represents the given convex data set defined over the interval $[a, b]$ where $a = u_0 < u_1 < u_2 < \dots < u_n = b$ and $d_j; j = 0, 1, 2, \dots, n$ designates the derivative values at the point $u_j; j = 0, 1, 2, \dots, n$.

Also, let

$$\check{\Delta}_j = \frac{v_{j+1} - v_j}{h_j}.$$

Additionally, the following condition is fulfilled by the derivative values:

$$\check{\Delta}_j \leq \check{\Delta}_{j+1}$$

$$d_j \leq d_{j+1}, d_j \leq \check{\Delta}_j \leq d_{j+1},$$

ϱ_j and σ_j are the parameters in the interval $[u_j, u_{j+1}]$.

The piecewise rational cubic function $T_j(u)$ defined in Eq. (2.1) is convex, if

$$T_j^{(2)}(u) \geq 0, u_0 \leq u \leq u_n$$

The value of $T_j^{(2)}(u)$ is computed as follows:

$$T_j^{(2)}(u) = \frac{\sum_{j=0}^5 (1-\xi)^{5-j} \xi^j \hat{a}_j}{h_j (Q_j(\xi))^3}, \quad (4.1)$$

where

$$\hat{a}_0 = 2\varrho_j^2 \sigma_j \check{\Delta}_j + 4\varrho_j^2 \check{\Delta}_j - 2\varrho_j^2 \sigma_j d_{j+1} - 4\varrho_j^2 d_j,$$

$$\hat{a}_1 = -2\varrho_j \sigma_j d_{j+1} - 4\varrho_j d_j - 3\varrho_j \sigma_j d_j + 5\varrho_j \sigma_j \check{\Delta}_j + 4\varrho_j \check{\Delta}_j,$$

$$\begin{aligned} \hat{a}_2 = & 3\sigma_j^2 d_{j+1} - \varrho_j \sigma_j d_{j+1} - 2\varrho_j d_j - 6\varrho_j \sigma_j d_j + 7\varrho_j \sigma_j \check{\Delta}_j + 2\varrho_j \check{\Delta}_j - \\ & 3\varrho_j^2 \check{\Delta}_j, \end{aligned}$$

$$\hat{a}_3 = 6\varrho_j \sigma_j d_{j+1} + 2\sigma_j d_{j+1} - 3\varrho_j^2 d_j + \varrho_j \sigma_j d_j + 3\varrho_j^2 \check{\Delta}_j - 7\varrho_j \sigma_j \check{\Delta}_j - 2\sigma_j \check{\Delta}_j,$$

$$\hat{a}_4 = 3\varrho_j \sigma_j d_{j+1} + 4\sigma_j d_{j+1} + 2\varrho_j \sigma_j d_j - 5\varrho_j \sigma_j \check{\Delta}_j - 4\sigma_j \check{\Delta}_j,$$

$$\hat{a}_5 = -2\varrho_j \sigma_j^2 \check{\Delta}_j + 4\sigma_j^2 \check{\Delta}_j + 2\varrho_j \sigma_j^2 d_j + 4\sigma_j^2 d_{j+1}.$$

The denominator quantity $Q_j(\xi)$ in (9) is a cube quantity and is positive if

$$\varrho_j \geq 0, \quad \sigma_j \geq 0.$$

In addition to this, the requisite condition for convexity in each subinterval is given as:

$$\hat{a}_j \geq 0; \quad j = 0, 1, 2, 3, 5.$$

After numerous manipulations, we successfully procure the constraints on σ_j and ϱ_j given by

$$\sigma_j > \max \left\{ 0, \frac{2(d_j - \check{\Delta}_j)}{(-d_{j+1} - 6d_j + 7\check{\Delta}_j)} \right\} \quad (4.2)$$

$$\varrho_j > \max \left\{ 0, \frac{2(\check{\Delta}_j - d_{j+1})}{(d_j + 6d_{j+1} - 7\check{\Delta}_j)} \right\} \quad (4.3)$$

which can be rearranged as

$$\sigma_j = \kappa_j + \max \left\{ 0, \frac{2(d_j - \check{\Delta}_j)}{(-d_{j+1} - 6d_j + 7\check{\Delta}_j)} \right\}, \quad \kappa_j > 0$$

$$\varrho_j = \varepsilon_j + \max \left\{ 0, \frac{2(\check{\Delta}_j - d_{j+1})}{(d_j + 6d_{j+1} - 7\check{\Delta}_j)} \right\}, \quad \varepsilon_j > 0$$

The above discussion is summarized as:

Theorem 1: Assume that $\{(u_j, v_j); j = 0, 1, 2, \dots, n\}$ be a convex data set. Then, the convexity is sustained by the piecewise rational cubic function defined in (1), if in each subinterval $[u_j, u_{j+1}], j = 0, 1, 2, \dots, n$ the parameters σ_j, ϱ_j satisfy the conditions :

$$\sigma_j = \kappa_j + \max \left\{ 0, \frac{2(d_j - \tilde{\Delta}_j)}{(-d_{j+1} - 6d_j + 7\tilde{\Delta}_j)} \right\}, \quad \kappa_j > 0$$

$$\varrho_j = \varepsilon_j + \max \left\{ 0, \frac{2(\tilde{\Delta}_j - d_{j+1})}{(d_j + 6d_{j+1} - 7\tilde{\Delta}_j)} \right\}. \quad \varepsilon_j > 0$$

5. CONVEX SURFACE MODEL

Consider a convex data set $\{(u_j, v_l, \tilde{G}_{j,l}); j = 0, 1, 2, \dots, n, l = 0, 1, 2, \dots, m\}$ demarcated over the rectangular mesh $[u_j, u_{j+1}] \times [v_j, v_{j+1}]$ for $j = 0, 1, 2, \dots, n-1, l = 0, 1, 2, \dots, m-1$ such that the following necessary conditions for convexity are settled:

$$\tilde{\Delta}_{j,l} \leq \tilde{\Delta}_{j+1,l}, \quad \tilde{G}_{j,l}^u \leq \tilde{G}_{j+1,l}^u, \quad \tilde{\Delta}_{j,l} \leq \tilde{\Delta}_{j,l+1}, \quad \tilde{G}_{j,l}^v \leq \tilde{G}_{j,l+1}^v$$

$$\tilde{\Delta}_{j,l} = \frac{\tilde{G}_{j+1,l} - \tilde{G}_{j,l}}{h_j}, \quad \tilde{\Delta}_{j,l} = \frac{\tilde{G}_{j,l+1} - \tilde{G}_{j,l}}{h_l}$$

$$\tilde{G}_{j,l}^u \leq \tilde{\Delta}_{j,l} \leq \tilde{G}_{j+1,l}^u, \quad \tilde{G}_{j,l}^v \leq \tilde{\Delta}_{j,l} \leq \tilde{G}_{j,l+1}^v$$

Now, convexity for the surface patch defined in (3.1) holds if all the boundary curves (3.3), (3.4), (3.5) and (3.6) are convex.

Consequently, the boundary curve $T(u, v_l)$ is convex if $T_j^{(2)}(u, v_l) \geq 0$ i.e.,

$$T_j^{(2)}(u, v_l) = \frac{\sum_{l=0}^5 (1-\xi)^{5-l} \xi^l \hat{b}_l}{h_j(Q_1(\xi))^3}, \quad (5.1)$$

where

$$\hat{b}_0 = 2\varrho_{j,l}^2 \sigma_{j,l} \tilde{\Delta}_{j,l} + 4\varrho_{j,l}^2 \tilde{\Delta}_{j,l} - 2\varrho_{j,l}^2 \sigma_{j,l} \tilde{G}_{j+1,l}^u - 4\varrho_{j,l}^2 \tilde{G}_{j,l}^u,$$

$$\hat{b}_1 = -2\varrho_{j,l} \sigma_{j,l} \tilde{G}_{j+1,l}^u - 4\varrho_{j,l} \tilde{G}_{j,l}^u - 3\varrho_{j,l} \sigma_{j,l} \tilde{G}_{j,l}^u + 5\varrho_{j,l} \sigma_{j,l} \tilde{\Delta}_{j,l} + 4\varrho_{j,l} \tilde{\Delta}_{j,l},$$

$$\hat{b}_2 = 3\sigma_{j,l}^2 \tilde{G}_{j+1,l}^u - \varrho_{j,l} \sigma_{j,l} \tilde{G}_{j+1,l}^u - 2\varrho_{j,l} \tilde{G}_{j,l}^u - 6\varrho_{j,l} \sigma_{j,l} \tilde{G}_{j,l}^u + 7\varrho_{j,l} \sigma_{j,l} \tilde{\Delta}_{j,l} + 2\varrho_{j,l} \tilde{\Delta}_{j,l} - 3\sigma_{j,l}^2 \tilde{\Delta}_{j,l},$$

$$\hat{b}_3 = 6\varrho_{j,l} \sigma_{j,l} \tilde{G}_{j+1,l}^u + 2\sigma_{j,l} \tilde{G}_{j+1,l}^u - 3\varrho_{j,l}^2 \tilde{G}_{j,l}^u + \varrho_{j,l} \sigma_{j,l} \tilde{G}_{j,l}^u + 3\varrho_{j,l}^2 \tilde{\Delta}_{j,l} - 7\varrho_{j,l} \sigma_{j,l} \tilde{\Delta}_{j,l} - 2\sigma_{j,l} \tilde{\Delta}_{j,l},$$

$$\hat{b}_4 = 3\varrho_{j,l} \sigma_{j,l} \tilde{G}_{j+1,l}^u + 4\sigma_{j,l} \tilde{G}_{j+1,l}^u + 2\varrho_{j,l} \sigma_{j,l} \tilde{G}_{j,l}^u - 5\varrho_{j,l} \sigma_{j,l} \tilde{\Delta}_{j,l} - 4\sigma_{j,l} \tilde{\Delta}_{j,l},$$

$$\hat{b}_5 = -2\varrho_{j,l} \sigma_{j,l}^2 \tilde{\Delta}_{j,l} + 4\sigma_{j,l}^2 \tilde{\Delta}_{j,l} + 2\varrho_{j,l} \sigma_{j,l}^2 \tilde{G}_{j,l}^u + 4\sigma_{j,l}^2 \tilde{G}_{j+1,l}^u.$$

Now, for positive $T_j^{(2)}(u, v_l)$, the numerator $\sum_{l=0}^5 (1 - \xi)^{5-l} \xi^l \hat{b}_l \geq 0$,

If

$$\hat{b}_l \geq 0, l = 0, 1, 2, 3, 4, 5$$

After frequent calculations, following constraints were inferred,

$$\sigma_{j,l} > \max \left\{ 0, \frac{2(\tilde{G}_{j,l}^u - \tilde{\Delta}_{j,l})}{(-\tilde{G}_{j+1,l}^u - 6\tilde{G}_{j,l}^u + 7\tilde{\Delta}_{j,l})} \right\},$$

$$\varrho_{j,l} > \max \left\{ 0, \frac{2(\tilde{\Delta}_{j,l} - \tilde{G}_{j+1,l}^u)}{(\tilde{G}_{j,l}^u + 6\tilde{G}_{j+1,l}^u - 7\tilde{\Delta}_{j,l})} \right\},$$

Correspondingly, $T(u, v_{l+1})$ is convex if $T_j^{(2)}(u, v_{l+1}) \geq 0$ i.e.,

$$T_j^{(2)}(u, v_{l+1}) = \frac{\sum_{l=0}^5 (1 - \xi)^{5-l} \xi^l \hat{c}_l}{h_j(Q_2(\xi))^3}, \quad (5.2)$$

where

$$\hat{c}_0 = 2\varrho_{j,l+1}^2 \sigma_{j,l+1} \tilde{\Delta}_{j,l+1} + 4\varrho_{j,l+1}^2 \tilde{\Delta}_{j,l+1} - 2\varrho_{j,l+1}^2 \sigma_{j,l+1} \tilde{G}_{j+1,l+1}^u - 4\varrho_{j,l+1}^2 \tilde{G}_{j,l+1}^u,$$

$$\hat{c}_1 = -2\varrho_{j,l+1} \sigma_{j,l+1} \tilde{G}_{j+1,l+1}^u - 4\varrho_{j,l+1} \tilde{G}_{j,l+1}^u - 3\varrho_{j,l+1} \sigma_{j,l+1} \tilde{G}_{j,l+1}^u + 5\varrho_{j,l+1} \sigma_{j,l+1} \tilde{\Delta}_{j,l+1} + 4\varrho_{j,l+1} \tilde{\Delta}_{j,l+1},$$

$$\hat{c}_2 = 3\sigma_{j,l+1}^2 \tilde{G}_{j+1,l+1}^u - \varrho_{j,l+1} \sigma_{j,l+1} \tilde{G}_{j+1,l+1}^u - 2\varrho_{j,l+1} \tilde{G}_{j,l+1}^u - 6\varrho_{j,l+1} \sigma_{j,l+1} \tilde{G}_{j,l+1}^u + 7\varrho_{j,l+1} \sigma_{j,l+1} \tilde{\Delta}_{j,l+1} + 2\varrho_{j,l+1} \tilde{\Delta}_{j,l+1} - 3\sigma_{j,l+1}^2 \tilde{\Delta}_{j,l+1},$$

$$\hat{c}_3 = 6\varrho_{j,l+1} \sigma_{j,l+1} \tilde{G}_{j+1,l+1}^u + 2\sigma_{j,l+1} \tilde{G}_{j+1,l+1}^u - 3\varrho_{j,l+1}^2 \tilde{G}_{j,l+1}^u + \varrho_{j,l+1} \sigma_{j,l+1} \tilde{G}_{j,l+1}^u + 3\varrho_{j,l+1}^2 \tilde{\Delta}_{j,l+1} - 7\varrho_{j,l+1} \sigma_{j,l+1} \tilde{\Delta}_{j,l+1} - 2\sigma_{j,l+1} \tilde{\Delta}_{j,l+1},$$

$$\hat{c}_4 = 3\varrho_{j,l+1} \sigma_{j,l+1} \tilde{G}_{j+1,l+1}^u + 4\sigma_{j,l+1} \tilde{G}_{j+1,l+1}^u + 2\varrho_{j,l+1} \sigma_{j,l+1} \tilde{G}_{j,l+1}^u - 5\varrho_{j,l+1} \sigma_{j,l+1} \tilde{\Delta}_{j,l+1} - 4\sigma_{j,l+1} \tilde{\Delta}_{j,l+1},$$

$$\hat{c}_5 = -2\varrho_{j,l+1} \sigma_{j,l+1}^2 \tilde{\Delta}_{j,l+1} + 4\sigma_{j,l+1}^2 \tilde{\Delta}_{j,l+1} + 2\varrho_{j,l+1} \sigma_{j,l+1}^2 \tilde{G}_{j,l+1}^u + 4\sigma_{j,l+1}^2 \tilde{G}_{j+1,l+1}^u.$$

For the numerator $\sum_{l=0}^5 (1 - \xi)^{5-l} \xi^l \hat{c}_l \geq 0$,

We must have

$$\hat{c}_l \geq 0, l = 0, 1, 2, 3, 4, 5.$$

which yields,

$$\begin{aligned}\sigma_{j,l+1} &> \max \left\{ 0, \frac{2(\tilde{G}_{j,l+1}^u - \tilde{\Delta}_{j,l+1})}{(-\tilde{G}_{j+1,l+1}^u - 6\tilde{G}_{j,l+1}^u + 7\tilde{\Delta}_{j,l+1})} \right\}, \\ \varrho_{j,l+1} &> \max \left\{ 0, \frac{2(\tilde{\Delta}_{j,l+1} - \tilde{G}_{j+1,l+1}^u)}{(\tilde{G}_{j,l+1}^u + 6\tilde{G}_{j+1,l+1}^u - 7\tilde{\Delta}_{j,l+1})} \right\}.\end{aligned}$$

Identically, $T(u_j, v)$ is convex if $T_j^{(2)}(u_j, v) \geq 0$ i.e.,

$$T_j^{(2)}(u_j, v) = \frac{\sum_{j=0}^5 (1-\xi)^{5-j} \xi^j \hat{r}_j}{\bar{h}_l(Q_3(\xi))^3}, \quad (5.3)$$

where

$$\begin{aligned}\hat{r}_0 &= 2\bar{\varrho}_{j,l}^2 \bar{\sigma}_{j,l} \tilde{\Delta}_{j,l} + 4\bar{\varrho}_{j,l}^2 \tilde{\Delta}_{j,l} - 2\bar{\varrho}_{j,l}^2 \bar{\sigma}_{j,l} \tilde{G}_{j,l+1}^v - 4\bar{\varrho}_{j,l}^2 \tilde{G}_{j,l}^v, \\ \hat{r}_1 &= -2\bar{\varrho}_{j,l} \bar{\sigma}_{j,l} \tilde{G}_{j,l+1}^v - 4\bar{\varrho}_{j,l} \bar{\sigma}_{j,l} \tilde{G}_{j,l}^v - 3\bar{\varrho}_{j,l} \bar{\sigma}_{j,l} \tilde{G}_{j,l}^v + 5\bar{\varrho}_{j,l} \bar{\sigma}_{j,l} \tilde{\Delta}_{j,l} + 4\bar{\varrho}_{j,l} \tilde{\Delta}_{j,l}, \\ \hat{r}_2 &= 3\bar{\varrho}_{j,l}^2 \tilde{G}_{j,l+1}^v - \bar{\varrho}_{j,l} \bar{\sigma}_{j,l} \tilde{G}_{j,l+1}^v - 2\bar{\varrho}_{j,l} \tilde{G}_{j,l}^v - 6\bar{\varrho}_{j,l} \bar{\sigma}_{j,l} \tilde{G}_{j,l}^v + 7\bar{\varrho}_{j,l} \bar{\sigma}_{j,l} \tilde{\Delta}_{j,l} + 2\bar{\varrho}_{j,l} \tilde{\Delta}_{j,l} - 3\bar{\varrho}_{j,l}^2 \tilde{\Delta}_{j,l}, \\ \hat{r}_3 &= 6\bar{\varrho}_{j,l} \bar{\sigma}_{j,l} \tilde{G}_{j,l+1}^v + 2\bar{\sigma}_{j,l} \tilde{G}_{j,l+1}^v - 3\bar{\varrho}_{j,l}^2 \tilde{G}_{j,l}^v + \bar{\varrho}_{j,l} \bar{\sigma}_{j,l} \tilde{G}_{j,l}^v + 3\bar{\varrho}_{j,l}^2 \tilde{\Delta}_{j,l} - 7\bar{\varrho}_{j,l} \bar{\sigma}_{j,l} \tilde{\Delta}_{j,l} - 2\bar{\sigma}_{j,l} \tilde{\Delta}_{j,l}, \\ \hat{r}_4 &= 3\bar{\varrho}_{j,l} \bar{\sigma}_{j,l} \tilde{G}_{j,l+1}^v + 4\bar{\sigma}_{j,l} \tilde{G}_{j,l+1}^v + 2\bar{\varrho}_{j,l} \bar{\sigma}_{j,l} \tilde{G}_{j,l}^v - 5\bar{\varrho}_{j,l} \bar{\sigma}_{j,l} \tilde{\Delta}_{j,l} - 4\bar{\sigma}_{j,l} \tilde{\Delta}_{j,l}, \\ \hat{r}_5 &= -2\bar{\varrho}_{j,l} \bar{\sigma}_{j,l}^2 \tilde{\Delta}_{j,l} + 4\bar{\sigma}_{j,l}^2 \tilde{\Delta}_{j,l} + 2\bar{\varrho}_{j,l} \bar{\sigma}_{j,l}^2 \tilde{G}_{j,l}^v + 4\bar{\sigma}_{j,l}^2 \tilde{G}_{j,l+1}^v.\end{aligned}$$

$$\text{Likewise, } \sum_{j=0}^5 (1-\xi)^{5-j} \xi^j \hat{r}_j \geq 0,$$

if

$$\hat{r}_j \geq 0; j = 0, 1, 2, 3, 4, 5.$$

This provides the following constraints,

$$\begin{aligned}\bar{\sigma}_{j,l} &> \max \left\{ 0, \frac{2(\tilde{G}_{j,l}^v - \tilde{\Delta}_{j,l})}{(-\tilde{G}_{j,l+1}^v - 6\tilde{G}_{j,l}^v + 7\tilde{\Delta}_{j,l})} \right\}, \\ \bar{\varrho}_{j,l} &> \max \left\{ 0, \frac{2(\tilde{\Delta}_{j,l} - \tilde{G}_{j,l+1}^v)}{(\tilde{G}_{j,l}^v + 6\tilde{G}_{j,l+1}^v - 7\tilde{\Delta}_{j,l})} \right\}.\end{aligned}$$

Eventually, $T(u_{j+1}, v)$ is convex if $T_j^{(2)}(u_{j+1}, v) \geq 0$ i.e.,

$$T_j^{(2)}(u_{j+1}, v) = \frac{\sum_{j=0}^5 (1-\xi)^{5-j} \xi^j \hat{s}_j}{\bar{h}_l(Q_4(\xi))^3}, \quad (5.4)$$

where

$$\begin{aligned} \hat{s}_0 &= 2\bar{\varrho}_{j+1,l}^2 \bar{\sigma}_{j+1,l} \bar{\Delta}_{j+1,l} + 4\bar{\varrho}_{j+1,l}^2 \bar{\Delta}_{j+1,l} - 2\bar{\varrho}_{j+1,l}^2 \bar{\sigma}_{j+1,l} \tilde{G}_{j+1,l+1}^v - \\ &\quad 4\bar{\varrho}_{j+1,l}^2 \tilde{G}_{j+1,l}^v, \\ \hat{s}_1 &= -2\bar{\varrho}_{j+1,l} \bar{\sigma}_{j+1,l} \tilde{G}_{j+1,l+1}^v - 4\bar{\varrho}_{j+1,l} \tilde{G}_{j+1,l}^v - 3\bar{\varrho}_{j+1,l} \bar{\sigma}_{j+1,l} \tilde{G}_{j+1,l}^v + \\ &\quad 5\bar{\varrho}_{j+1,l} \bar{\sigma}_{j+1,l} \bar{\Delta}_{j+1,l} + 4\bar{\varrho}_{j+1,l} \bar{\Delta}_{j+1,l}, \\ \hat{s}_2 &= 3\bar{\varrho}_{j+1,l}^2 \tilde{G}_{j+1,l+1}^v - \bar{\varrho}_{j+1,l} \bar{\sigma}_{j+1,l} \tilde{G}_{j+1,l+1}^v - 2\bar{\varrho}_{j+1,l} \tilde{G}_{j+1,l}^v - \\ &\quad 6\bar{\varrho}_{j+1,l} \bar{\sigma}_{j+1,l} \tilde{G}_{j+1,l}^v + 7\bar{\varrho}_{j+1,l} \bar{\sigma}_{j+1,l} \bar{\Delta}_{j+1,l} + 2\bar{\varrho}_{j+1,l} \bar{\Delta}_{j+1,l} - 3\bar{\varrho}_{j+1,l}^2 \bar{\Delta}_{j+1,l}, \\ \hat{s}_3 &= 6\bar{\varrho}_{j+1,l} \bar{\sigma}_{j+1,l} \tilde{G}_{j+1,l+1}^v + 2\bar{\sigma}_{j+1,l} \tilde{G}_{j+1,l+1}^v - 3\bar{\varrho}_{j+1,l}^2 \tilde{G}_{j+1,l}^v + \\ &\quad \bar{\varrho}_{j+1,l} \bar{\sigma}_{j+1,l} \tilde{G}_{j+1,l}^v + 3\bar{\varrho}_{j+1,l}^2 \bar{\Delta}_{j+1,l} - 7\bar{\varrho}_{j+1,l} \bar{\sigma}_{j+1,l} \bar{\Delta}_{j+1,l} - 2\bar{\sigma}_{j+1,l} \bar{\Delta}_{j+1,l}, \\ \hat{s}_4 &= 3\bar{\varrho}_{j+1,l} \bar{\sigma}_{j+1,l} \tilde{G}_{j+1,l+1}^v + 4\bar{\sigma}_{j+1,l} \tilde{G}_{j+1,l+1}^v + 2\bar{\varrho}_{j+1,l} \bar{\sigma}_{j+1,l} \tilde{G}_{j+1,l}^v - \\ &\quad 5\bar{\varrho}_{j+1,l} \bar{\sigma}_{j+1,l} \bar{\Delta}_{j+1,l} - 4\bar{\sigma}_{j+1,l} \bar{\Delta}_{j+1,l}, \\ \hat{s}_5 &= -2\bar{\varrho}_{j+1,l} \bar{\sigma}_{j+1,l}^2 \bar{\Delta}_{j+1,l} + 4\bar{\sigma}_{j+1,l}^2 \bar{\Delta}_{j+1,l} + 2\bar{\varrho}_{j+1,l} \bar{\sigma}_{j+1,l}^2 \tilde{G}_{j+1,l}^v + \\ &\quad 4\bar{\sigma}_{j+1,l}^2 \tilde{G}_{j+1,l+1}^v. \end{aligned}$$

Likewise, $\sum_{j=0}^5 (1-\xi)^{5-j} \xi^j \hat{s}_j \geq 0$, if

$$\hat{s}_j \geq 0; j = 0, 1, 2, 3, 4, 5$$

This provides the following constraints,

$$\bar{\sigma}_{j+1,l} > \max \left\{ 0, \frac{2(\tilde{G}_{j+1,l}^v - \bar{\Delta}_{j+1,l})}{(-\tilde{G}_{j+1,l+1}^v - 6\tilde{G}_{j+1,l}^v + 7\bar{\Delta}_{j+1,l})} \right\},$$

$$\bar{\varrho}_{j+1,l} > \max \left\{ 0, \frac{2(\bar{\Delta}_{j+1,l} - \tilde{G}_{j+1,l+1}^v)}{(\tilde{G}_{j+1,l}^v + 6\tilde{G}_{j+1,l+1}^v - 7\bar{\Delta}_{j+1,l})} \right\}.$$

This discussion is briefed as:

Theorem 2: The visualization of 3D convex data as convex surface for Bi-cubic partially blended rational function in (3) can be rendered if in each rectangular mesh $I = [u_j, u_{j+1}] \times [v_l, v_{l+1}]$, the parameters

$\varrho_{j,l}, \sigma_{j,l}, \varrho_{j,l+1}, \sigma_{j,l+1}, \bar{\varrho}_{j,l}, \bar{\sigma}_{j,l}, \bar{\varrho}_{j+1,l}, \bar{\sigma}_{j+1,l}$, assure the following constraints:

$$\begin{aligned}\sigma_{j,l} &> \max \left\{ 0, \frac{2(\tilde{G}_{j,l}^u - \tilde{\Delta}_{j,l})}{(-\tilde{G}_{j+1,l}^u - 6\tilde{G}_{j,l}^u + 7\tilde{\Delta}_{j,l})} \right\}, \quad \varrho_{j,l} > \max \left\{ 0, \frac{2(\tilde{\Delta}_{j,l} - \tilde{G}_{j+1,l}^u)}{(\tilde{G}_{j,l}^u + 6\tilde{G}_{j+1,l}^u - 7\tilde{\Delta}_{j,l})} \right\}, \\ \sigma_{j,l+1} &> \max \left\{ 0, \frac{2(\tilde{G}_{j,l+1}^u - \tilde{\Delta}_{j,l+1})}{(-\tilde{G}_{j+1,l+1}^u - 6\tilde{G}_{j,l+1}^u + 7\tilde{\Delta}_{j,l+1})} \right\}, \\ \varrho_{j,l+1} &> \max \left\{ 0, \frac{2(\tilde{\Delta}_{j,l+1} - \tilde{G}_{j+1,l+1}^u)}{(\tilde{G}_{j,l+1}^u + 6\tilde{G}_{j+1,l+1}^u - 7\tilde{\Delta}_{j,l+1})} \right\}, \\ \bar{\sigma}_{j,l} &> \max \left\{ 0, \frac{2(\tilde{G}_{j,l}^v - \tilde{\Delta}_{j,l})}{(-\tilde{G}_{j+1,l}^v - 6\tilde{G}_{j,l}^v + 7\tilde{\Delta}_{j,l})} \right\}, \quad \bar{\varrho}_{j,l} > \max \left\{ 0, \frac{2(\tilde{\Delta}_{j,l} - \tilde{G}_{j+1,l}^v)}{(\tilde{G}_{j,l}^v + 6\tilde{G}_{j+1,l}^v - 7\tilde{\Delta}_{j,l})} \right\}, \\ \bar{\sigma}_{j+1,l} &> \max \left\{ 0, \frac{2(\tilde{G}_{j+1,l}^v - \tilde{\Delta}_{j+1,l})}{(-\tilde{G}_{j+1,l+1}^v - 6\tilde{G}_{j+1,l}^v + 7\tilde{\Delta}_{j+1,l})} \right\}, \\ \bar{\varrho}_{j+1,l} &> \max \left\{ 0, \frac{2(\tilde{\Delta}_{j+1,l} - \tilde{G}_{j+1,l+1}^v)}{(\tilde{G}_{j+1,l}^v + 6\tilde{G}_{j+1,l+1}^v - 7\tilde{\Delta}_{j+1,l})} \right\}.\end{aligned}$$

Adjusting the above constraints as:

$$\begin{aligned}\sigma_{j,l} &= a_{j,l} + \max \left\{ 0, \frac{2(\tilde{G}_{j,l}^u - \tilde{\Delta}_{j,l})}{(-\tilde{G}_{j+1,l}^u - 6\tilde{G}_{j,l}^u + 7\tilde{\Delta}_{j,l})} \right\}, \quad a_{j,l} > 0 \\ \varrho_{j,l} &= b_{j,l} + \max \left\{ 0, \frac{2(\tilde{\Delta}_{j,l} - \tilde{G}_{j+1,l}^u)}{(\tilde{G}_{j,l}^u + 6\tilde{G}_{j+1,l}^u - 7\tilde{\Delta}_{j,l})} \right\}, \quad b_{j,l} > 0 \\ \sigma_{j,l+1} &= c_{j,l} + \max \left\{ 0, \frac{2(\tilde{G}_{j,l+1}^u - \tilde{\Delta}_{j,l+1})}{(-\tilde{G}_{j+1,l+1}^u - 6\tilde{G}_{j,l+1}^u + 7\tilde{\Delta}_{j,l+1})} \right\}, \quad c_{j,l} > 0 \\ \varrho_{j,l+1} &= d_{j,l} + \max \left\{ 0, \frac{2(\tilde{\Delta}_{j,l+1} - \tilde{G}_{j+1,l+1}^u)}{(\tilde{G}_{j,l+1}^u + 6\tilde{G}_{j+1,l+1}^u - 7\tilde{\Delta}_{j,l+1})} \right\}, \quad d_{j,l} > 0 \\ \bar{\sigma}_{j,l} &= e_{j,l} + \max \left\{ 0, \frac{2(\tilde{G}_{j,l}^v - \tilde{\Delta}_{j,l})}{(-\tilde{G}_{j+1,l}^v - 6\tilde{G}_{j,l}^v + 7\tilde{\Delta}_{j,l})} \right\}, \quad e_{j,l} > 0 \\ \bar{\varrho}_{j,l} &= g_{j,l} + \max \left\{ 0, \frac{2(\tilde{\Delta}_{j,l} - \tilde{G}_{j+1,l}^v)}{(\tilde{G}_{j,l}^v + 6\tilde{G}_{j+1,l}^v - 7\tilde{\Delta}_{j,l})} \right\}, \quad g_{j,l} > 0\end{aligned}$$

$$\bar{\sigma}_{j+1,l} = m_{j,l} + \max \left\{ 0, \frac{2(\tilde{G}_{j+1,l}^v - \check{\Delta}_{j+1,l})}{(-\tilde{G}_{j+1,l+1}^v - 6\tilde{G}_{j+1,l}^v + 7\check{\Delta}_{j+1,l})} \right\}, \quad m_{j,l} > 0$$

$$\bar{\varrho}_{j+1,l} = n_{j,l} + \max \left\{ 0, \frac{2(\check{\Delta}_{j+1,l} - \tilde{G}_{j+1,l+1}^v)}{(\tilde{G}_{j+1,l}^v + 6\tilde{G}_{j+1,l+1}^v - 7\check{\Delta}_{j+1,l})} \right\}. \quad n_{j,l} > 0$$

6. RESULTS AND DISCUSSIONS

This section describes algorithm for the proposed shape preserving techniques in section 4 and verify its effectiveness through graphical results in the subsequent numerical examples.

6.1. Algorithm. Convex Curve Model

Step 1: Compute $(n + 1)$ convex data points $\{(u_j, v_j); j = 0, 1, 2, \dots, n\}$

Step 2: Approximate the derivatives $\check{\Delta}_j$ at the notes using Arithmetic mean method.

Step 3: Using Theorem 1, evaluate free parameters σ_j and ϱ_j .

Step 4: Insert the above values in Eq. (4.1).

Example 1. The data in Table 1 encloses convex data set. MATLAB programming software packet was used to implement constraints on shape parameter in order to visualize convex curve. Numerical results were recorded in Table 5. Figure 1 clearly reflects the shape characteristic of convexity.

Table 1. A Convex 2D Data Set

u_i	-3	-2	-1	0	1	2	3	4	5
v_i	17	10	5	1.8	1	1.8	5	10	17

Example 2. Another convex data set was considered to implement the proposed algorithm using MATLAB software packet and results are shown in Table 6, while Figure 2 clearly depicts convexity of data.

Table 2. A Convex 2D Data Set

u_i	1	2	3	4	4.9	6
v_i	4.11	9.39	20.3	54.2	163.89	438.1

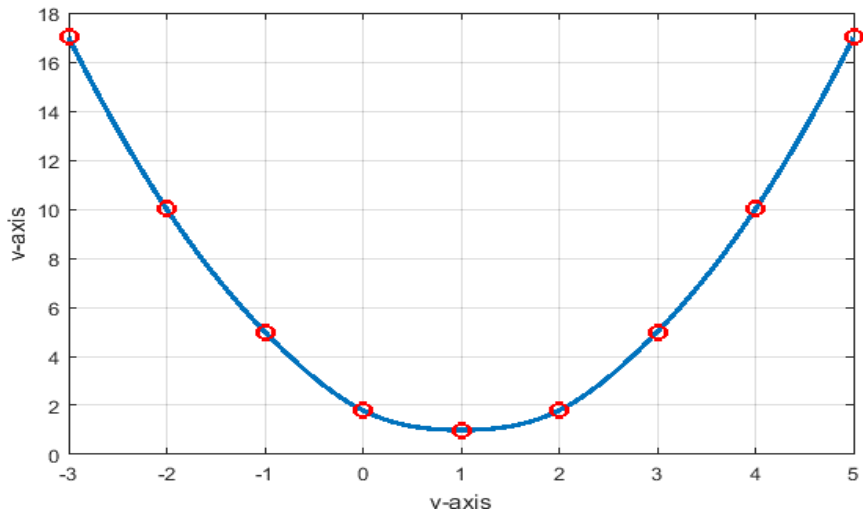


Figure 1. Convexity Preserving Curve of Convex 2D Data Set in Table 1 Using Convex Rational Cubic Spline Function

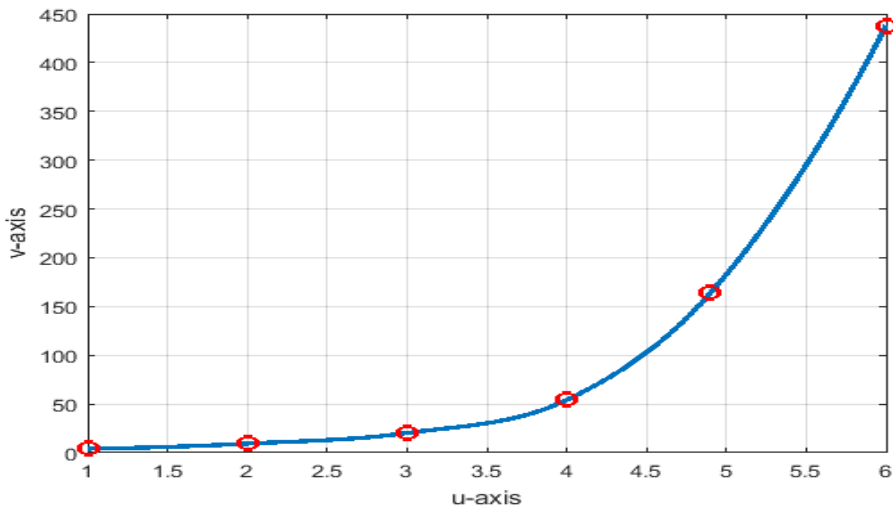


Figure 2. A Convex Curve of Data Set taken in Table 2 Using Convex Rational Cubic Spline Function

Algorithm 2. Convex Surface Model

Step 1: Compute $(n + 1) \times (m + 1)$ convex data point points $\{(u_j, v_j, \tilde{G}_{j,l}): j = 0, 1, 2, \dots, n; l = 0, 1, 2, \dots, m\}$.

Step 2: Approximate the derivatives $\tilde{G}_{j,l}^u$ and $\tilde{G}_{j,l}^v$ at the notes using Arithmetic mean method.

Step 3: Using Theorem 2, evaluate free parameters $\varrho_{j,l}$, $\sigma_{j,l}$, $\varrho_{j,l+1}$, $\sigma_{j,l+1}$, $\bar{\varrho}_{j,l}$, $\bar{\sigma}_{j,l}$, $\bar{\varrho}_{j+1,l}$ and $\bar{\sigma}_{j+1,l}$.

Step 4: Insert the above values in (3).

Example 3. A convex 3D data set is prescribed in Table 3 which is created by the function particularized in the following Eq. (6.1). Convexity is conserved by utilizing convex bi-cubic rational function with the graphical representation illustrated in Figure 3. Numerical results are displayed in Table 7. The uz-view and the vz-view of the convex surface is given in the Figure 4 and Figure 5, respectively.

$$\tilde{G}(u, v) = u^2 + v^2 + 0.1. \quad (6.1)$$

Table 3. A Convex 3D Data set

<i>u/v</i>	-5	-4	-3	-2	-1	0	1	2	3	4	5	6
-5	50.1	41.1	34.1	29.1	26.1	25.1	26.1	29.1	34.1	41.1	50.1	61.1
-4	41.1	32.1	25.1	20.1	17.1	16.1	17.1	20.1	25.1	32.1	41.1	52.1
-3	34.1	25.1	18.1	13.1	10.1	9.1	10.1	13.1	18.1	25.1	34.1	45.1
-2	29.1	20.1	13.1	8.1	5.1	4.1	5.1	8.1	13.1	20.1	29.1	40.1
-1	26.1	17.1	10.1	5.1	2.1	1.1	2.1	5.1	10.1	17.1	26.1	37.1
0	25.1	16.1	9.1	4.1	1.1	0.1	1.1	4.1	9.1	16.1	25.1	36.1
1	26.1	17.1	10.1	5.1	2.1	1.1	2.1	5.1	10.1	17.1	26.1	37.1
2	29.1	20.1	13.1	8.1	5.1	4.1	5.1	8.1	13.1	20.1	29.1	40.1
3	34.1	25.1	18.1	13.1	10.1	9.1	10.1	13.1	18.1	25.1	34.1	45.1
4	41.1	32.1	25.1	20.1	17.1	16.1	17.1	20.1	25.1	32.1	41.1	52.1
5	50.1	50.1	41.1	34.1	29.1	26.1	25.1	26.1	29.1	34.1	41.1	50.1
6	61.1	52.1	45.1	40.1	37.1	36.1	37.1	40.1	45.1	52.1	61.1	72.1

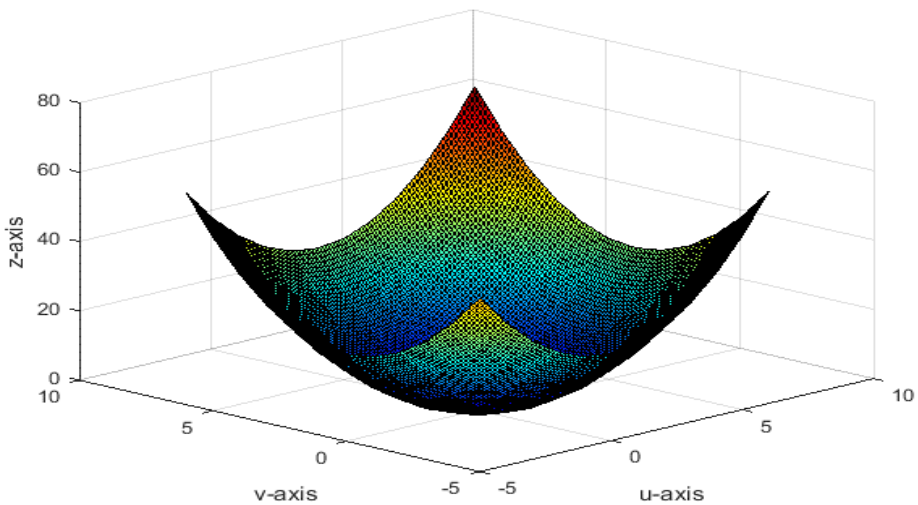


Figure 3. A Convex Surface produced from the Convex Data Set in Table 3

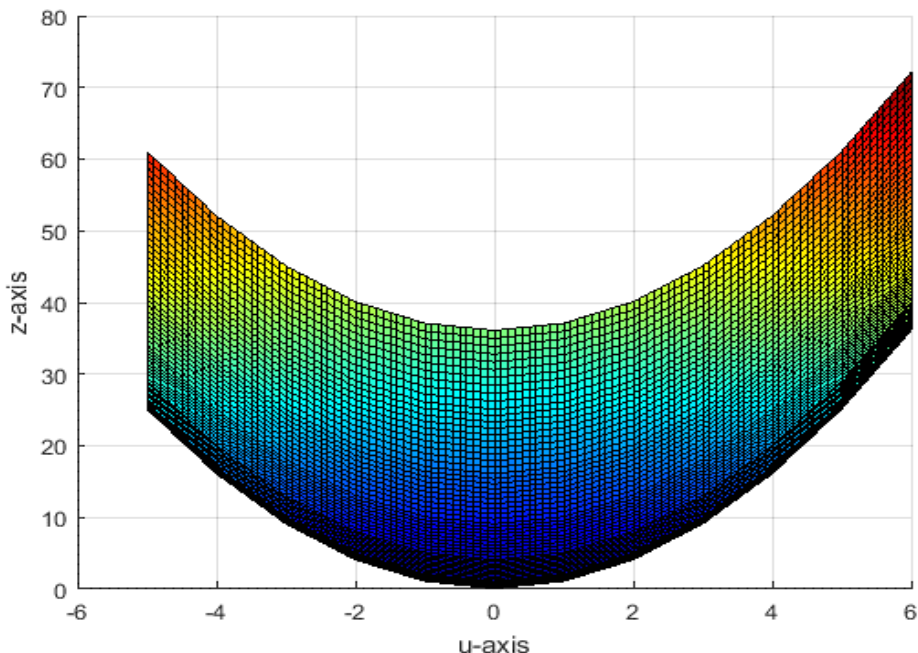
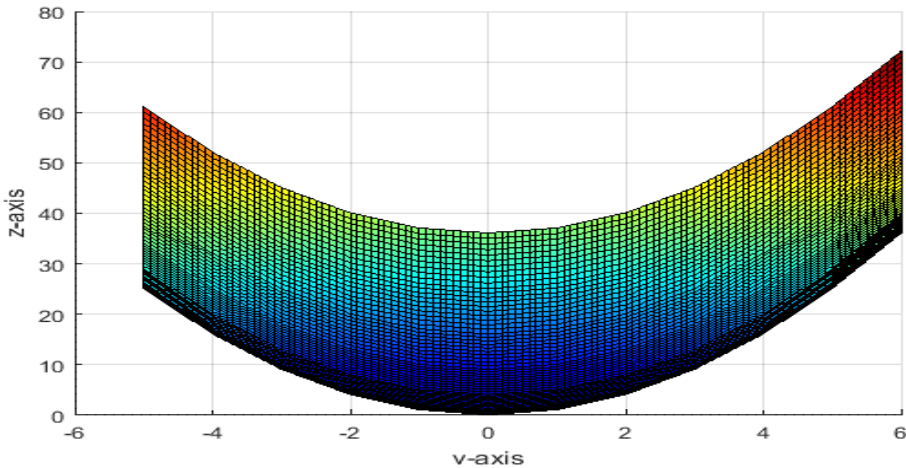


Figure 4. A uz-view of the Convex Surface

**Figure 5.** A vz-view of the Convex Surface

Example 4. Another convex 3D data set in Table 4 is made up by the function given by the subsequent equation (17). The convex rational bi-cubic functions help to preserve the convexity of the data which can be visualized in Figure 6. Figures 7, and Figure 8 give the uz-view and vz-view of the convex surface, respectively. Numerical results are shown in Table 8.

$$\tilde{G}(u, v) = (u^2 + v^2 - 1)^2 + 0.2. \quad (6.2)$$

Table 4. A Convex 3D Data set

<i>u/v</i>	0	1	2	3	4	5	6	7
0	1.2	0.2	9.2	64.2	225.2	576.2	1225.2	2304.2
1	0.2	1.2	16.2	81.2	256.2	625.2	1296.2	2401.2
2	9.2	16.2	49.2	144.2	361.2	784.2	1521.2	2704.2
3	64.2	81.2	144.2	289.2	576.2	1089.2	1936.2	3249.2
4	225.2	256.2	361.2	576.2	961.2	1600.2	2601.2	4096.2
5	576.2	625.2	784.2	1089.2	1600.2	2401.2	3600.2	5329.2
6	1225.2	1296.2	1521.2	1936.2	2601.2	3600.2	5041.2	7056.2
7	2304.2	2401.2	2704.2	3249.2	4096.2	5329.2	7056.2	9409.2

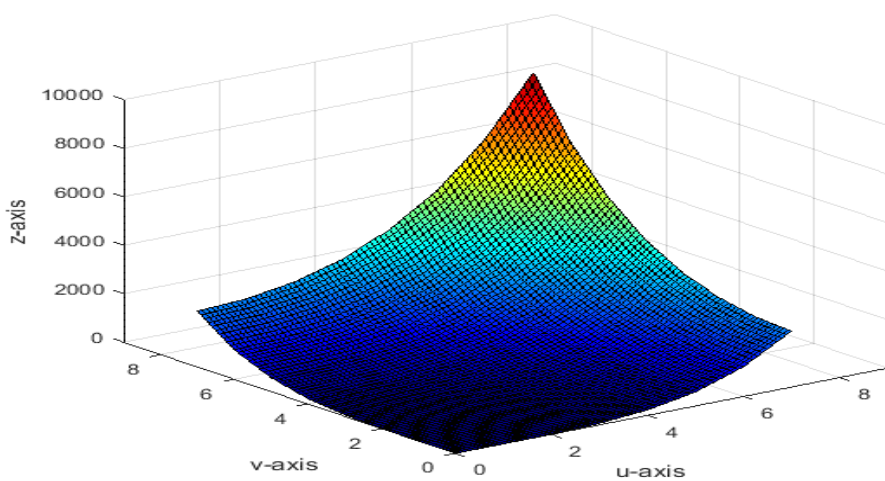


Figure 6. A Convex Surface Constructed from the Convex Data set in Table 4

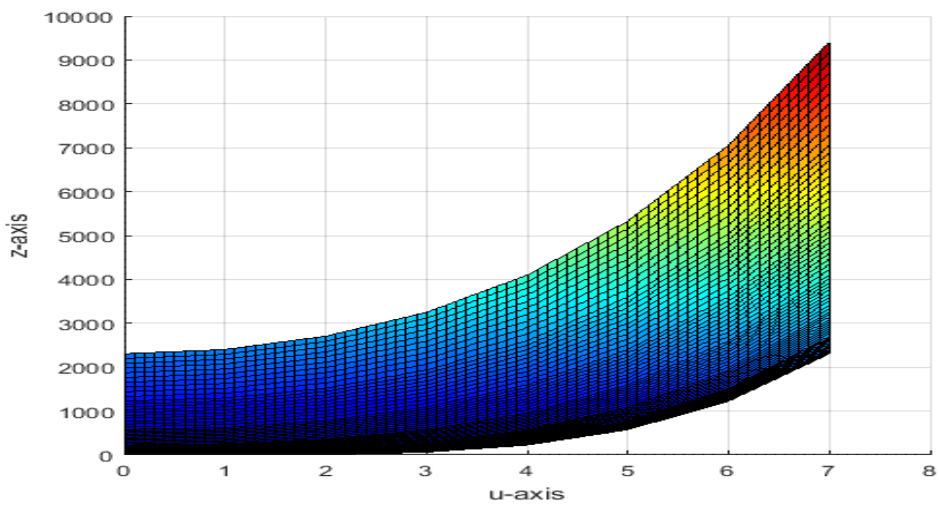


Figure 7. A *uz*-view of the Convex Surface

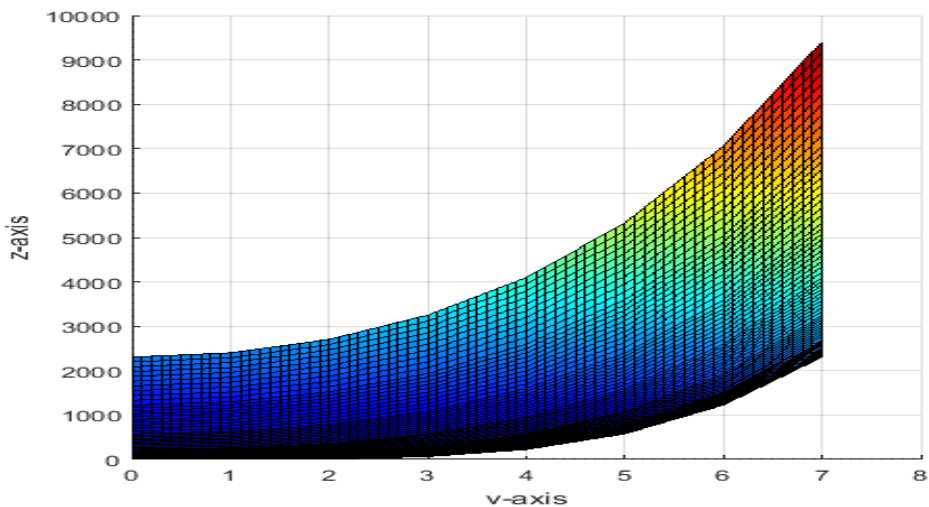


Figure 8. A vz-view of the Convex Surface

7. NUMERICAL RESULTS

This section presents the numerical results when proposed algorithm was implemented on 2D convex data set in Table 1 and Table 2. Similarly, for 3D convex data in Table 3 and Table 4, numerical results are given in Table 7 and Table 8. MATLAB software packets were used for programming and visualizing convex curves and surfaces.

Table 5. Numerical Results Parallel to Figure 1

i	1	2	3	4	5	6	7	8	9
d_i	-8.000	-6.000	-4.100	-2.000	0	2.000	4.100	6.000	8.000
ϱ_i	1	1	1	1	1	1	1	1	—
σ_i	1	1	1	1	1	1	1	1	—

Table 6. Numerical Results for Figure 2

i	1	2	3	4	5	6
d_i	2.4650	8.0950	22.4050	77.8889	185.5798	319.3540
ϱ_i	1	1	1	1	1	—
σ_i	1	1	1	1	1	—

Table 7. Numerical Results for Figure 3

u/v	-5	-4	-3	-2	-1	0	1	2	3	4	5	6
Numerical results for $\tilde{G}_{j,l}^u$												
-5	-10.0	-10.0	-10.0	-10.0	-10.0	-10.0	-10.0	-10.0	-10.0	-10.0	-10.0	-10.0
-4	-8.00	-8.00	-8.00	-8.00	-8.00	-8.00	-8.00	-8.00	-8.00	-8.00	-8.00	-8.00
-3	-6.00	-6.00	-6.00	-6.00	-6.00	-6.00	-6.00	-6.00	-6.00	-6.00	-6.00	-6.00
-2	-4.00	-4.00	-4.00	-4.00	-4.00	-4.00	-4.00	-4.00	-4.00	-4.00	-4.00	-4.00
-1	-2.00	-2.00	-2.00	-2.00	-2.00	-2.00	-2.00	-2.00	-2.00	-2.00	-2.00	-2.00
0	0	0	0	0	0	0	0	0	0	0	0	0
1	2.00	2.00	2.00	2.00	2.00	2.00	2.00	2.00	2.00	2.00	2.00	2.00
2	4.00	4.00	4.00	4.00	4.00	4.00	4.00	4.00	4.00	4.00	4.00	4.00
3	6.00	6.00	6.00	6.00	6.00	6.00	6.00	6.00	6.00	6.00	6.00	6.00
4	8.00	8.00	8.00	8.00	8.00	8.00	8.00	8.00	8.00	8.00	8.00	8.00
5	10.0	10.0	10.0	10.0	10.0	10.0	10.0	10.0	10.0	10.0	10.0	10.0
6	12.0	12.0	12.0	12.0	12.0	12.0	12.0	12.0	12.0	12.0	12.0	12.0
Numerical results for $\tilde{G}_{j,l}^v$												
-5	-10.0	-8.00	-6.00	-4.00	-2.00	0	2.00	4.00	6.00	8.00	10.0	12.0
-4	-10.0	-8.00	-6.00	-4.00	-2.00	0	2.00	4.00	6.00	8.00	10.0	12.0
-3	-10.0	-8.00	-6.00	-4.00	-2.00	0	2.00	4.00	6.00	8.00	10.0	12.0

u/v	-5	-4	-3	-2	-1	0	1	2	3	4	5	6
-2	-10.0	-8.00	-6.00	-4.00	-2.00	0	2.00	4.00	6.00	8.00	10.0	12.0
-1	-10.0	-8.00	-6.00	-4.00	-2.00	0	2.00	4.00	6.00	8.00	10.0	12.0
0	-10.0	-8.00	-6.00	-4.00	-2.00	0	2.00	4.00	6.00	8.00	10.0	12.0
1	-10.0	-8.00	-6.00	-4.00	-2.00	0	2.00	4.00	6.00	8.00	10.0	12.0
2	-10.0	-8.00	-6.00	-4.00	-2.00	0	2.00	4.00	6.00	8.00	10.0	12.0
3	-10.0	-8.00	-6.00	-4.00	-2.00	0	2.00	4.00	6.00	8.00	10.0	12.0
4	-10.0	-8.00	-6.00	-4.00	-2.00	0	2.00	4.00	6.00	8.00	10.0	12.0
5	-10.0	-8.00	-6.00	-4.00	-2.00	0	2.00	4.00	6.00	8.00	10.0	12.0
6	-10.0	-8.00	-6.00	-4.00	-2.00	0	2.00	4.00	6.00	8.00	10.0	12.0
Numerical results for $\varrho_{j,l}$												
-5	1.00	1.00	1.00	1.00	1.000	1.000	1.000	1.000	1.000	1.000	1.000	—
-4	1.000	1.000	1.000	1.000	1.000	1.000	1.000	1.000	1.000	1.000	1.000	—
-3	1.000	1.000	1.000	1.000	1.000	1.000	1.000	1.000	1.000	1.000	1.000	—
-2	1.000	1.000	1.000	1.000	1.000	1.000	1.000	1.000	1.000	1.000	1.000	—
-1	1.000	1.000	1.000	1.000	1.000	1.000	1.000	1.000	1.000	1.000	1.000	—
0	1.000	1.000	1.000	1.000	1.000	1.000	1.000	1.000	1.000	1.000	1.000	—
1	1.000	1.000	1.000	1.000	1.000	1.000	1.000	1.000	1.000	1.000	1.000	—
2	1.000	1.000	1.000	1.000	1.000	1.000	1.000	1.000	1.000	1.000	1.000	—

u/v	-5	-4	-3	-2	-1	0	1	2	3	4	5	6
3	1.000	1.000	1.000	1.000	1.000	1.000	1.000	1.000	1.000	1.000	1.000	—
4	1.000	1.000	1.000	1.000	1.000	1.000	1.000	1.000	1.000	1.000	1.000	—
5	1.000	1.000	1.000	1.000	1.000	1.000	1.000	1.000	1.000	1.000	1.000	—
6	—	—	—	—	—	—	—	—	—	—	—	—
Numerical results for $\sigma_{j,l}$												
-5	1.000	1.000	1.000	1.000	1.000	1.000	1.000	1.000	1.000	1.000	1.000	—
-4	1.000	1.000	1.000	1.000	1.000	1.000	1.000	1.000	1.000	1.000	1.000	—
-3	1.000	1.000	1.000	1.000	1.000	1.000	1.000	1.000	1.000	1.000	1.000	—
-2	1.000	1.000	1.000	1.000	1.000	1.000	1.000	1.000	1.000	1.000	1.000	—
-1	1.000	1.000	1.000	1.000	1.000	1.000	1.000	1.000	1.000	1.000	1.000	—
0	1.000	1.000	1.000	1.000	1.000	1.000	1.000	1.000	1.000	1.000	1.000	—
1	1.000	1.000	1.000	1.000	1.000	1.000	1.000	1.000	1.000	1.000	1.000	—
2	1.000	1.000	1.000	1.000	1.000	1.000	1.000	1.000	1.000	1.000	1.000	—
3	1.000	1.000	1.000	1.000	1.000	1.000	1.000	1.000	1.000	1.000	1.000	—
4	1.000	1.000	1.000	1.000	1.000	1.000	1.000	1.000	1.000	1.000	1.000	—
5	1.000	1.000	1.000	1.000	1.000	1.000	1.000	1.000	1.000	1.000	1.000	—
6	—	—	—	—	—	—	—	—	—	—	—	—
Numerical results for $\varrho_{j,l+1}$												

Shape-Preserving Curve...

u/v	-5	-4	-3	-2	-1	0	1	2	3	4	5	6
-5	1.000	1.000	1.000	1.000	1.000	1.000	1.000	1.000	1.000	1.000	1.000	—
-4	1.000	1.000	1.000	1.000	1.000	1.000	1.000	1.000	1.000	1.000	1.000	—
-3	1.000	1.000	1.000	1.000	1.000	1.000	1.000	1.000	1.000	1.000	1.000	—
-2	1.000	1.000	1.000	1.000	1.000	1.000	1.000	1.000	1.000	1.000	1.000	—
-1	1.000	1.000	1.000	1.000	1.000	1.000	1.000	1.000	1.000	1.000	1.000	—
0	1.000	1.000	1.000	1.000	1.000	1.000	1.000	1.000	1.000	1.000	1.000	—
1	1.000	1.000	1.000	1.000	1.000	1.000	1.000	1.000	1.000	1.000	1.000	—
2	1.000	1.000	1.000	1.000	1.000	1.000	1.000	1.000	1.000	1.000	1.000	—
3	1.000	1.000	1.000	1.000	1.000	1.000	1.000	1.000	1.000	1.000	1.000	—
4	1.000	1.000	1.000	1.000	1.000	1.000	1.000	1.000	1.000	1.000	1.000	—
5	1.000	1.000	1.000	1.000	1.000	1.000	1.000	1.000	1.000	1.000	1.000	—
6	—	—	—	—	—	—	—	—	—	—	—	—
Numerical results for $\sigma_{j,l+1}$												
-5	1.000	1.000	1.000	1.000	1.000	1.000	1.000	1.000	1.000	1.000	1.000	—
-4	1.000	1.000	1.000	1.000	1.000	1.000	1.000	1.000	1.000	1.000	1.000	—
-3	1.000	1.000	1.000	1.000	1.000	1.000	1.000	1.000	1.000	1.000	1.000	—
-2	1.000	1.000	1.000	1.000	1.000	1.000	1.000	1.000	1.000	1.000	1.000	—
-1	1.000	1.000	1.000	1.000	1.000	1.000	1.000	1.000	1.000	1.000	1.000	—

u/v	-5	-4	-3	-2	-1	0	1	2	3	4	5	6
0	1.000	1.000	1.000	1.000	1.000	1.000	1.000	1.000	1.000	1.000	1.000	—
1	1.000	1.000	1.000	1.000	1.000	1.000	1.000	1.000	1.000	1.000	1.000	—
2	1.000	1.000	1.000	1.000	1.000	1.000	1.000	1.000	1.000	1.000	1.000	—
3	1.000	1.000	1.000	1.000	1.000	1.000	1.000	1.000	1.000	1.000	1.000	—
4	1.000	1.000	1.000	1.000	1.000	1.000	1.000	1.000	1.000	1.000	1.000	—
5	1.000	1.000	1.000	1.000	1.000	1.000	1.000	1.000	1.000	1.000	1.000	—
6	—	—	—	—	—	—	—	—	—	—	—	—
Numerical results for $\bar{q}_{j,l}$												
-5	1.000	1.000	1.000	1.000	1.000	1.000	1.000	1.000	1.000	1.000	1.000	—
-4	1.000	1.000	1.000	1.000	1.000	1.000	1.000	1.000	1.000	1.000	1.000	—
-3	1.000	1.000	1.000	1.000	1.000	1.000	1.000	1.000	1.000	1.000	1.000	—
-2	1.000	1.000	1.000	1.000	1.000	1.000	1.000	1.000	1.000	1.000	1.000	—
-1	1.000	1.000	1.000	1.000	1.000	1.000	1.000	1.000	1.000	1.000	1.000	—
0	1.000	1.000	1.000	1.000	1.000	1.000	1.000	1.000	1.000	1.000	1.000	—
1	1.000	1.000	1.000	1.000	1.000	1.000	1.000	1.000	1.000	1.000	1.000	—
2	1.000	1.000	1.000	1.000	1.000	1.000	1.000	1.000	1.000	1.000	1.000	—
3	1.000	1.000	1.000	1.000	1.000	1.000	1.000	1.000	1.000	1.000	1.000	—
4	1.000	1.000	1.000	1.000	1.000	1.000	1.000	1.000	1.000	1.000	1.000	—

u/v	-5	-4	-3	-2	-1	0	1	2	3	4	5	6
5	1.000	1.000	1.000	1.000	1.000	1.000	1.000	1.000	1.000	1.000	1.000	—
6	—	—	—	—	—	—	—	—	—	—	—	—
Numerical results for $\bar{\sigma}_{j,l}$												
-5	1.000	1.000	1.000	1.000	1.000	1.000	1.000	1.000	1.000	1.000	1.000	—
-4	1.000	1.000	1.000	1.000	1.000	1.000	1.000	1.000	1.000	1.000	1.000	—
-3	1.000	1.000	1.000	1.000	1.000	1.000	1.000	1.000	1.000	1.000	1.000	—
-2	1.000	1.000	1.000	1.000	1.000	1.000	1.000	1.000	1.000	1.000	1.000	—
-1	1.000	1.000	1.000	1.000	1.000	1.000	1.000	1.000	1.000	1.000	1.000	—
0	1.000	1.000	1.000	1.000	1.000	1.000	1.000	1.000	1.000	1.000	1.000	—
1	1.000	1.000	1.000	1.000	1.000	1.000	1.000	1.000	1.000	1.000	1.000	—
2	1.000	1.000	1.000	1.000	1.000	1.000	1.000	1.000	1.000	1.000	1.000	—
3	1.000	1.000	1.000	1.000	1.000	1.000	1.000	1.000	1.000	1.000	1.000	—
4	1.000	1.000	1.000	1.000	1.000	1.000	1.000	1.000	1.000	1.000	1.000	—
5	1.000	1.000	1.000	1.000	1.000	1.000	1.000	1.000	1.000	1.000	1.000	—
6	—	—	—	—	—	—	—	—	—	—	—	—
Numerical results for $\bar{\varrho}_{j+1,l}$												
-5	1.000	1.000	1.000	1.000	1.000	1.000	1.000	1.000	1.000	1.000	1.000	—
-4	1.000	1.000	1.000	1.000	1.000	1.000	1.000	1.000	1.000	1.000	1.000	—

u/v	-5	-4	-3	-2	-1	0	1	2	3	4	5	6
-3	1.000	1.000	1.000	1.000	1.000	1.000	1.000	1.000	1.000	1.000	1.000	—
-2	1.000	1.000	1.000	1.000	1.000	1.000	1.000	1.000	1.000	1.000	1.000	—
-1	1.000	1.000	1.000	1.000	1.000	1.000	1.000	1.000	1.000	1.000	1.000	—
0	1.000	1.000	1.000	1.000	1.000	1.000	1.000	1.000	1.000	1.000	1.000	—
1	1.000	1.000	1.000	1.000	1.000	1.000	1.000	1.000	1.000	1.000	1.000	—
2	1.000	1.000	1.000	1.000	1.000	1.000	1.000	1.000	1.000	1.000	1.000	—
3	1.000	1.000	1.000	1.000	1.000	1.000	1.000	1.000	1.000	1.000	1.000	—
4	1.000	1.000	1.000	1.000	1.000	1.000	1.000	1.000	1.000	1.000	1.000	—
5	1.000	1.000	1.000	1.000	1.000	1.000	1.000	1.000	1.000	1.000	1.000	—
6	—	—	—	—	—	—	—	—	—	—	—	—
Numerical results for $\bar{\sigma}_{j+1,l}$												
-5	1.000	1.000	1.000	1.000	1.000	1.000	1.000	1.000	1.000	1.000	1.000	—
-4	1.000	1.000	1.000	1.000	1.000	1.000	1.000	1.000	1.000	1.000	1.000	—
-3	1.000	1.000	1.000	1.000	1.000	1.000	1.000	1.000	1.000	1.000	1.000	—
-2	1.000	1.000	1.000	1.000	1.000	1.000	1.000	1.000	1.000	1.000	1.000	—
-1	1.000	1.000	1.000	1.000	1.000	1.000	1.000	1.000	1.000	1.000	1.000	—
0	1.000	1.000	1.000	1.000	1.000	1.000	1.000	1.000	1.000	1.000	1.000	—
1	1.000	1.000	1.000	1.000	1.000	1.000	1.000	1.000	1.000	1.000	1.000	—

u/v	-5	-4	-3	-2	-1	0	1	2	3	4	5	6
2	1.000	1.000	1.000	1.000	1.000	1.000	1.000	1.000	1.000	1.000	1.000	—
3	1.000	1.000	1.000	1.000	1.000	1.000	1.000	1.000	1.000	1.000	1.000	—
4	1.000	1.000	1.000	1.000	1.000	1.000	1.000	1.000	1.000	1.000	1.000	—
5	1.000	1.000	1.000	1.000	1.000	1.000	1.000	1.000	1.000	1.000	1.000	—
6	—	—	—	—	—	—	—	—	—	—	—	—

Table 8. Numerical Results for Figure 4

u/v	0	1	2	3	4	5	6	7
Numerical Results for $\tilde{G}_{j,l}^u$								
0	-0.0060	-0.0060	-0.0060	-0.0060	-0.0060	-0.0060	-0.0060	-0.0060
1	0.0040	0.0080	0.0200	0.0400	0.0680	0.1040	0.1480	0.2000
2	0.0320	0.0400	0.0640	0.1040	0.1600	0.2320	0.3200	0.4240
3	0.1080	0.1200	0.1560	0.2160	0.3000	0.4080	0.5400	0.6960
4	0.2560	0.2720	0.3200	0.4000	0.5120	0.6560	0.8320	1.0400
5	0.5000	0.5200	0.5800	0.6800	0.8200	1.000	1.2200	1.4800
6	0.8640	0.8880	0.9600	1.0800	1.2480	1.4640	1.7280	2.0400
7	1.2940	1.3220	1.4060	1.5640	1.7420	1.9940	2.3020	2.6660
Numerical Results for $\tilde{G}_{j,l}^v$								
0	-0.0060	0.0040	0.0320	0.1080	0.2560	0.5000	0.8640	1.2940
1	-0.0060	0.0080	0.0400	0.1200	0.2720	0.5200	0.8880	1.3220
2	-0.0060	0.0200	0.0640	0.1560	0.3200	0.5800	0.9600	1.4060
3	-0.0060	0.0400	0.1040	0.2160	0.4000	0.6800	1.0800	1.5460

u/v	0	1	2	3	4	5	6	7
4	-0.0060	0.0680	0.1600	0.3000	0.5120	0.8200	1.2480	1.7420
5	-0.0060	0.1040	0.2320	0.4080	0.6560	1.000	1.4640	1.9940
6	-0.0060	0.1480	0.3200	0.5400	0.8320	1.2200	1.7280	2.3020
7	-0.0060	0.2000	0.4240	0.6960	1.0400	1.4800	2.0400	2.6660
Numerical results for $\varrho_{j,l}$								
0	1.000	1.000	1.000	1.000	1.000	1.000	1.000	—
1	1.000	1.000	1.000	1.000	1.000	1.000	1.000	—
2	1.000	1.000	1.000	1.000	1.000	1.000	1.000	—
3	1.000	1.000	1.000	1.000	1.000	1.000	1.000	—
4	1.000	1.000	1.000	1.000	1.000	1.000	1.000	—
5	1.000	1.000	1.000	1.000	1.000	1.000	1.000	—
6	1.000	1.000	1.000	1.000	1.000	1.000	1.000	—
7	—	—	—	—	—	—	—	—
Numerical results for $\sigma_{j,l}$								
0	1.000	1.000	1.000	1.000	1.000	1.000	1.000	—
1	1.000	1.000	1.000	1.000	1.000	1.000	1.000	—
2	1.000	1.000	1.000	1.000	1.000	1.000	1.000	—
3	1.000	1.000	1.000	1.000	1.000	1.000	1.000	—
4	1.000	1.000	1.000	1.000	1.000	1.000	1.000	—
5	1.000	1.000	1.000	1.000	1.000	1.000	1.000	—
6	1.000	1.000	1.000	1.000	1.000	1.000	1.000	—
7	—	—	—	—	—	—	—	—
Numerical results for $\varrho_{j,l+1}$								
0	1.000	1.000	1.000	1.000	1.000	1.000	1.000	—

u/v	0	1	2	3	4	5	6	7
1	1.000	1.000	1.000	1.000	1.000	1.000	1.000	—
2	1.000	1.000	1.000	1.000	1.000	1.000	1.000	—
3	1.000	1.000	1.000	1.000	1.000	1.000	1.000	—
4	1.000	1.000	1.000	1.000	1.000	1.000	1.000	—
5	1.000	1.000	1.000	1.000	1.000	1.000	1.000	—
6	1.000	1.000	1.000	1.000	1.000	1.000	1.000	—
7	—	—	—	—	—	—	—	—
Numerical results for $\sigma_{j,l+1}$								
0	1.000	1.000	1.000	1.000	1.000	1.000	1.000	—
1	1.000	1.000	1.000	1.000	1.000	1.000	1.000	—
2	1.000	1.000	1.000	1.000	1.000	1.000	1.000	—
3	1.000	1.000	1.000	1.000	1.000	1.000	1.000	—
4	1.000	1.000	1.000	1.000	1.000	1.000	1.000	—
5	1.000	1.000	1.000	1.000	1.000	1.000	1.000	—
6	1.000	1.000	1.000	1.000	1.000	1.000	1.000	—
7	—	—	—	—	—	—	—	—
Numerical results for $\bar{q}_{j,l}$								
0	1.000	1.000	1.000	1.000	1.000	1.000	1.000	—
1	1.000	1.000	1.000	1.000	1.000	1.000	1.000	—
2	1.000	1.000	1.000	1.000	1.000	1.000	1.000	—
3	1.000	1.000	1.000	1.000	1.000	1.000	1.000	—
4	1.000	1.000	1.000	1.000	1.000	1.000	1.000	—
5	1.000	1.000	1.000	1.000	1.000	1.000	1.000	—
6	1.000	1.000	1.000	1.000	1.000	1.000	1.000	—

u/v	0	1	2	3	4	5	6	7
7	—	—	—	—	—	—	—	—
Numerical results for $\bar{\sigma}_{j,l}$								
0	1.000	1.000	1.000	1.000	1.000	1.000	1.000	—
1	1.000	1.000	1.000	1.000	1.000	1.000	1.000	—
2	1.000	1.000	1.000	1.000	1.000	1.000	1.000	—
3	1.000	1.000	1.000	1.000	1.000	1.000	1.000	—
4	1.000	1.000	1.000	1.000	1.000	1.000	1.000	—
5	1.000	1.000	1.000	1.000	1.000	1.000	1.000	—
6	1.000	1.000	1.000	1.000	1.000	1.000	1.000	—
7	—	—	—	—	—	—	—	—
Numerical results for $\bar{q}_{j+1,l}$								
0	1.000	1.000	1.000	1.000	1.000	1.000	1.000	—
1	1.000	1.000	1.000	1.000	1.000	1.000	1.000	—
2	1.000	1.000	1.000	1.000	1.000	1.000	1.000	—
3	1.000	1.000	1.000	1.000	1.000	1.000	1.000	—
4	1.000	1.000	1.000	1.000	1.000	1.000	1.000	—
5	1.000	1.000	1.000	1.000	1.000	1.000	1.000	—
6	1.000	1.000	1.000	1.000	1.000	1.000	1.000	—
7	—	—	—	—	—	—	—	—
Numerical results for $\bar{\sigma}_{j+1,l}$								
0	1.000	1.000	1.000	1.000	1.000	1.000	1.000	—
1	1.000	1.000	1.000	1.000	1.000	1.000	1.000	—
2	1.000	1.000	1.000	1.000	1.000	1.000	1.000	—
3	1.000	1.000	1.000	1.000	1.000	1.000	1.000	—

Shape-Preserving Curve...

u/v	0	1	2	3	4	5	6	7
4	1.000	1.000	1.000	1.000	1.000	1.000	1.000	—
5	1.000	1.000	1.000	1.000	1.000	1.000	1.000	—
6	1.000	1.000	1.000	1.000	1.000	1.000	1.000	—
7	—	—	—	—	—	—	—	—

8. CONCLUSION

In the current research, shape preserving rational schemes were devised for convex curve and surface data. A C^1 rational cubic piecewise function, composed of cubic numerator and quadratic denominator with two free parameters σ_j and ϱ_j , was used to retain the intrinsic shape characteristic of 2D convex data. Mathematical derivation was performed to derive the data dependent constraints on free parameter and results were summarized in Theorem 1. MATLAB software packet was used to implement the developed scheme and visualize 2D convex data. Furthermore, the function was then advanced to partially blended rational bi-cubic function with eight free parameters for the 3D convex data positioned over rectangular grid. These eight parameters $\sigma_{j,l}, \varrho_{j,l}, \sigma_{j,l+1}, \varrho_{j,l+1}, \bar{\sigma}_{j,l}, \bar{\varrho}_{j,l}, \bar{\sigma}_{j+1,l}$, and $\bar{\varrho}_{j+1,l}$ by means of mathematical derivation, were conditioned to preserve the inherent curvature of 3D data and findings were summarized in Theorem 2. The proposed algorithm controls the shape of visual model locally. Convex surfaces were realized with the help of MATLAB software packet. The suggested shape-preserving techniques in this study are applicable to both data and derivatives and do not alter basis functions. The proposed scheme, however, does not use free parameters which provides the users with minimal flexibility to change the shape of the data as they desire. Work on curvature preserving scheme for scatter data is in process by the authors.

REFERENCES

1. Ebrahimi AR, Loghmani GB, Sarfraz M. Capturing outlines of generic shapes with cubic Bézier curves using the Nelder–Mead simplex method. *Iran J Numer Anal Optim.* 2019;9(2):103–121. <https://doi.org/10.22067/IJNAO.V9I2.70045>
2. Ebrahimi AR, Loghmani GB, Sarfraz M. Capturing outlines of planar generic images by simultaneous curve fitting and sub-division. *J AI Data Mining.* 2020;8(1):105–118. <https://doi.org/10.22044/JADM.2019.6727.1788>
3. Ebrahimi AR, Loghmani GB. B-spline curve fitting by diagonal approximation BFGS methods. *Iran J Sci Technol Trans A.* 2019;43(3):947–958. <https://doi.org/10.1007/s40995-017-0347-1>
4. Jahanshahloo A, Ebrahimi AR. Reconstruction of 3D shapes with B-spline surface using diagonal approximation BFGS methods. *Multimed Tools Appl.* 2022;81:38091–38111. <https://doi.org/10.1007/s11042-022-13024-6>

5. Jahanshahloo A, Ebrahimi AR. Reconstruction of the initial curve from a two-dimensional shape for the B-spline curve fitting. *Eur Phys J Plus*. 2022;137:e411. <https://doi.org/10.1140/epjp/s13360-022-02604-y>
6. Kvasov BI. Monotone and convex interpolation by weighted quadratic splines. *Adv Comput Math.* 2014;40(1): 91–116. <https://doi.org/10.1007/s10444-013-9300-9>
7. Verlan I. Convexity preserving interpolation by splines of arbitrary degree. *Comput Sci J Mold.* 2010;18(1):54–58.
8. Clements JC. A convexity preserving parametric C^2 rational cubic interpolant. *Numer Math.* 1992;63(1):165–171. <https://doi.org/10.1007/BF01385853>
9. Merriam JL, Sablonniere P. Rational splines for hermite interpolation with shape constraints. *Comput Aided Geom Des.* 2013;30:296–309. <https://doi.org/10.1016/j.cagd.2013.01.004>
10. Carnicer JM, Garcia-Esnaol M, Peña JM. Convexity of rational curves and total positivity. *J Comput App Math.* 1996;71(2):365–382. [https://doi.org/10.1016/0377-0427\(95\)00240-5](https://doi.org/10.1016/0377-0427(95)00240-5)
11. Brodlie KW, Butt S. Preserving convexity using piecewise cubic interpolation. *Comput Graphs.* 1991;15:15–23. [https://doi.org/10.1016/0097-8493\(91\)90026-E](https://doi.org/10.1016/0097-8493(91)90026-E)
12. Hussain M, Hussain MZ, Waseem A, Javaid M. GC^1 Shape-preserving trigonometric surfaces. *J Math Imaging Vis.* 2015;53(1):21–41. <https://doi.org/10.1007/s10851-014-0544-x>
13. Sarfraz M, Hussain MZ, Nisar A. Positive data modelling using spline functions. *Appl Math Comput.* 2010;216:2036–2049. <https://doi.org/10.1016/j.amc.2010.03.034>
14. Sarfraz M, Hussain MZ, Hussain F. Shape preserving convex data interpolation. *Appl Comput Math.* 2017;16(3):205–227.
15. Sarfraz M, Hussain MZ, Hussain M. Shape preserving curve interpolation. *Int J of Comput Math.* 2012;89(1):35–53. <https://doi.org/10.1080/00207160.2011.627434>
16. Tian M, Li SL. Convexity-Preserving piecewise rational cubic interpolation. *J Shand Univ.* 2007;42(10):80–83.
17. Floater MS. A weak condition for the convexity of tensor-product Bézier and B-spline surfaces. *Adv Comput Math.* 1994;2(1):67–80. <https://doi.org/10.1007/BF02519036>

18. Hussain MZ, Hussain M, Waseem A. Shape-preserving trigonometric functions. *Comput App Math*. 2014;33:411–431. <https://doi.org/10.1007/s40314-013-0071-1>
19. Hussain MZ, Hussain M. Visualization of 3D data preserving convexity. *J App Math Comput*. 2006;2:170–186. <https://doi.org/10.1007/BF02831986>
20. Hussain MZ, Hussain M. Convex surface interpolation. In: Chen F, Jüttler B. eds., *Advances in Geometric Modeling and Processing. GMP 2008. Lecture Notes in Computer Science*. Springer, Berlin, Heidelberg. https://doi.org/10.1007/978-3-540-79246-8_36
21. Costantini P. On monotone and convex spline interpolation. *Math Comput*. 1986;46(173):203–214. <https://doi.org/10.2307/2008224>
22. Costantini P, Fontanella F. Shape preserving bivariate interpolation. *SIAM J Numer Anal*. 1990;27(2):488–506. <https://doi.org/10.1137/0727030>
23. Asatryan S. *Shape Preserving Surface Interpolation Scheme* [Doctoral dissertation]. University of Dundee; 1992.
24. Asatryan S, Costantini P, Manni C. Local shape preserving interpolation by space curves. *IMA J Numer Anal*. 2001;21(1):301–325. <https://doi.org/10.1093/imanum/21.1.301>
25. Dodd SL, McAllister DF, Roulier J. Shape-Preserving spline interpolation for specifying bivariate functions on grids. *IEEE Comput Graph App*. 1983;3(6):70–79.
26. Han X. Shape-preserving piecewise rational Interpolant with quartic numerator and quadratic denominator. *App Math Comput*. 2015;251:258–274. <https://doi.org/10.1016/j.amc.2014.11.067>